

Artificial intelligent techniques applied for detection COVID-19 based on chest medical imaging

Nawres Aref Alwash, Hussain Kareem Khleaf

Department of Electrical Engineering, College of Engineering, University of Technology, Baghdad, Iraq

Article Info

Article history:

Received Jun 11, 2021

Revised Feb 25, 2022

Accepted Mar 05, 2022

Keywords:

Artificial intelligence

COVID-19

FFBPN

Medical imaging

Rasperry pi

SVM

ABSTRACT

One of the ways to detect coronavirus disease of 2019 (COVID-19) is X-rays, computerized tomography (CT). This paper aims to detect COVID-19 from CT images without any user intervention. The proposed algorithm consists of 5 stages. These stages include; the first stage aims to collect data from hospitals and internet websites, the second stage is pre-processing stage to remove noise and convert it from red green blue (RGB) to grayscale and then improve image quality, the third is the segmentation stage which included threshold and region-growing segmentation methods. The fourth stage is used to extract important characteristics, and the last stage is classification CT images using feed forward back propagation network (FFBPN) and support vector machines (SVM) and compare the results between them and see if the person is infected or healthy. This study was implemented in MATLAB software. The results showed that the noise cancellation technology using anisotropic filtering gave the best results. Region-growing method was reliable to separate COVID-19 infected from healthy regions. The FFBPN has given the best results for detecting and classifying COVID-19. The results of the proposed methodology are rapid and accurate in detecting COVID-19. The output from classifier is displayed on the Rasperry Pi that included weather if patient is infected or not and the severity of COVID-19 infection.

This is an open access article under the [CC BY-SA](https://creativecommons.org/licenses/by-sa/4.0/) license.



Corresponding Author:

Nawres Aref Alwash

Department of Electrical Engineering, College of Engineering, University of Technology

Baghdad, Iraq

E-mail: eee.19.18@grad.uotechnology.edu.iq

1. INTRODUCTION

Coronavirus disease of 2019 (COVID-19) is close to a virus called severe acute respiratory syndrome coronavirus 2 (SARS-CoV-2) [1]. This virus quickly spread within 30 days [2], from Wuhan to all Chinese cities [3]. Then, to the United States of America [4]. These viruses infected animals [5], then transmitted to humans this virus SARS-CoV, known as middle east respiratory syndrome corona virus (MERS-CoV) [6], which infects the acute respiratory system and leads to human deaths [7]. Symptoms for this virus are cough, fatigue, fever, headache; body aches sore throat and shortness of breath [8]. Many contactless imaging techniques [9] have been developed during the outbreak of the COVID-19 virus [10], [11], including the use of the examination rooms [12] of surveillance cameras [13] or their use of the system [14] and then the use of portable computer tomography [15]. Automatic scanning with portable computerized tomography (CT) scanning platform supported with visual artificial intelligence techniques are a prime example [16], CT portable platform as shown in Figure 1(a) CT portable platform. By using a pre-screening system as well as a diagnostic system that relies mainly on the principle of artificial intelligence [17], this portable system works completely by itself. It was transferred to a survey room and then to a control room,

where it is completely isolated. Therefore, to prevent any unwanted contact between technicians and patients, every room has a private entrance. Where the patient is asked to stand on the patient's bed after entering the examination room, patient monitor camera as in the Figure 1(b) patient monitor camera. As for the technicians, they can look through the window, as well as make a survival video transmit from artificial intelligence (AI) camera installed in the ceiling of the scanning room, and also correct the patient's position if he needs, a technician determines the position and examines the patient as in Figure 1(c) a technician determines the position and examines the patient. The algorithm using to automatically determine a patient's position restoring 3D position and a patient's reconfigured grid from previous images in the camera [18] until the patient is ready, or through the technician or using an algorithm for motion analysis. The 3D grid does the job, in which the center line is 3D estimated for the fitness stage of the injured person and then converted into alerts for control as well as optimized scan parameters for the technician for the purpose of verification. Then, the technician can make some adjustments and then automatically align the patient's bed with the international organization for standardization (ISO) center and then transfer it to the CT bridge for scanning. For the purpose of obtaining the CT images, they are finally analyzed and processed for examination and diagnosis.

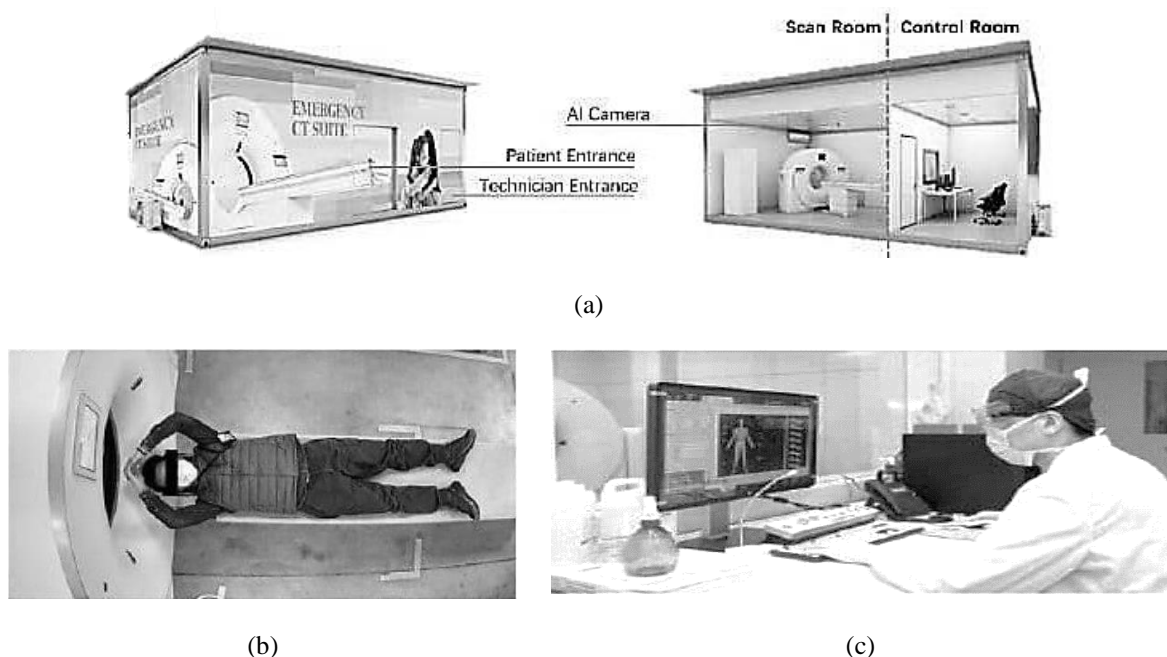


Figure 1: Scanner room components for: (a) CT portable platform, (b) patient monitor camera, and (c) a technician determines the position and examines the patient

Many researches using CT or X-ray for detection disease such as Khobragade *et al.* [19] the use of forward feeding of neural networks by chest radiography to detect artificial lung disease. This paper has suggested dividing the lung. In terms of extracting the lung feature. Using image processing techniques such as methods of severity and methods of discontinuity to detect lung boundaries, and the result extracted from statistical and engineering features and to determine if the patient has any lung disease such as tuberculosis, pneumonia and lung cancer, Prayogo *et al.* [20] this research used X-ray image using siamese convolutional networks for classification of pneumonia.

Khan *et al.* [21] CoroNet proposal, a deep convolutional neural network model for detecting COVID-19 infection from chest X-ray images. The proposed model is based on the pre-trained Xception architecture of the ImageNet dataset. The proposed model achieved an accuracy of 93% for COVID-19 cases and 98.2% for categories 4 cases (COVID-19 vs bacterial vs viral vs normal pneumonia). For the three categories (COVID-19 vs pneumonia vs normal) the initial results of this study appear promising and could be improved with more training data [21].

That is, applying carrier regression for COVID-19 cases, as well as to test the different structures using kernel function and analyze sensitivity of the predictive performance of the models for the purpose of preparing different meta-parameters when applying 3-laying the typeface. In this experiment the model used to give highest degree of nonlinearity (Gaussian kernel) and it gave best performance inside the sample,

but gave the worst predictions out of the sample, as this is an example for over processing in machines learning models. The efficiency of the linear kernel function was rather poor, but it gave the best predictions from the sample. In this paper we obtained the results of an empirical evaluation of the basic concept for the purpose of data analysis as well as presentation the need to exercise caution when applying models in machine learning for the purpose of supporting real-world decision-making, especially in the difficulties caused by the COVID-19 epidemics. Al-Ars and Al-Bakry [22] This paper used improving medical diagnosis by hybrid fuzzy logic and k-mean. Croock *et al.* [23] these reasearchers are discussed early diagnosis for breast cancer by mammography image and software engineering processes and good and satisfactory results are obtained.

2. METHODOLOGY

For details used at each stage of the proposed algorithms. Where the proposed algorithms consist of five stages for detecting COVID-19. These stages consist of the following: first collecting data from hospitals as real data as well as from the Internet (computerized tomography lung image), then the image processing stage to remove noise and convert the image from red green blue (RGB) to grayscale, after which the image improvement stage, then the segmentation stage, segmentation technology plays the primary role of image processing. Image segmentation divides the image into several regions where it corresponds to the objects and different parts of the objects. These results are used to extract quantitative information from the image, threshold, including clustering.

In this paper, the proposed algorithm and morphological processes affect the shape, structure or shape of an object. Applies to binary image (white and black) and pixels between (zero, one) [24]. They are used for pre or post preprocessing (thinning, clarification, and pruning) or in describing (borders, skeletons, convex bodies) [25]. The first step to remove unwanted pixels is by filling in the small hole of white pixels inside dark back-ground with the dark pixels and dark holes turn into a white pixel. Simple area-filling algorithm depending on specific expansions, integrations and intersections. The second step, erosion processes remove pixels from the objects' boundary region. The process of adding and removing pixels to the border area of objects depends on the image skeleton element. Region growing zone growth is a method of segmenting the picture depending on the area. It categorizes a pixel-based image segmentation method because it includes a selection of start point. The segmentation method examines a pixels adjacent to the start point and determines whether or not adjacent pixels should be added to the region. Thus, the process is repeated in the same way as general data-gathering algorithms.

Then feature extraction is extracting the input information and converting it into a feature set called feature vector, in which a function group extracts information from inputs data to perform a classification tasks. The purpose from this stage is to reduce the size of data that is used for AI networks, in order to increase efficiency of classification. This paper, tissue features by gray level co-occurrence matrix (GLCM) have been used to extract statistical feature. These features are employed for classification stage. The final stage is the classification of the CT images using feed forward back propagation network (FFBPN) and support vector machine (SVM) and compare the result between them and determine whether the person is infected or healthy.

2.1. Classification stage

Classification stage is to classify CT images into sets to identify COVID-19 by FFBPN is utilized for accomplish difficult tasks and several kinds for application because it is efficient, simple for using and the results are very good and SVM algorithms. In this paper feature extraction has been done by gray level co-occurrence matrix (GLCM) used for classification stage. The CT images are classified into (class 1) for non-COVID-19 images and (class 0) for COVID-19 images. FFBPN is used in this paper and it is considered one of the types of artificial neural networks because it is considered simple to use. The multi layer forward feeding process requires determining number for hidden layer and neuron in each layer, number for neurons of the input layer, types for activation function and number output layer.

2.1.1. Training of FFBPN algorithm

The CT image features are divided into two groups, test group and training set, for training performance for neural networks model. A percentage for image of CT features in the training set equals 70% of the total feature count and the percentage of features in the test set equals 30%. We need to determine number for hidden layer, type of communication between layer, number for neuron in each layers, and the neuronal activation functions in order to design a multi layer feeding network. Figure 2 illustrates the training for FFBPN. Neural network training is process of defining network parameters (biases, weights). When training process is completed for the training data set, the updated weights and bias values were saved in a

file to be ready for the testing procedure. The weights of the neural network are adapted with the help of a learning algorithm.

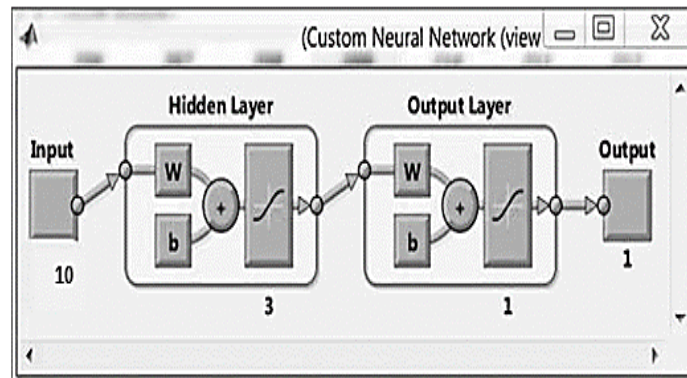


Figure 2: Training network for FFBN

2.1.2. SVM

SVM is also one of effective classification methods. It is a binary classifier; where the extracted feature fall into 2 groups. The SVM nonlinear classifier uses images defined by two sets (set 0 and set 1). In the COVID-19 CT images, set 1 is classified for COVID-19, and set 0 is classified for non-COVID-19. In this work, the corresponding output of the SVM classification. The results are shown in MATLAB for lung image it is a normal SVM classifier for CT images taken from information base for the states and show accuracy for SVM linear kernel.

3. EXPERIMENTAL DATA

The proposed algorithm is based on actual data from Kaggle website. which are 150 CT lung images case of train, 150 CT lung image cases of test. Also, through fieldwork to collect CT lung images case of train and 30% CT lung image case of test 70% from Al-Marjahn hospital, Babil-Iraq. Table 1 and Table 2 show details of the testing and training of the CT lung images and were used directly for pre-treatment and CT lung images taken from hospitals in compact disk (CD) format where the CT lung images were in digital imaging and communications in medicine (DICOM) (DCM) format (real CT lung images), and using an online website to convert the format photo and save as digital color Pictures in JPEG format on a computer.

Table 1. CT images training data sets

Classified of detection	Kaggle website	Al-Marjahn hospital	Total
Normal	50	20	70
Infected	15	5	20

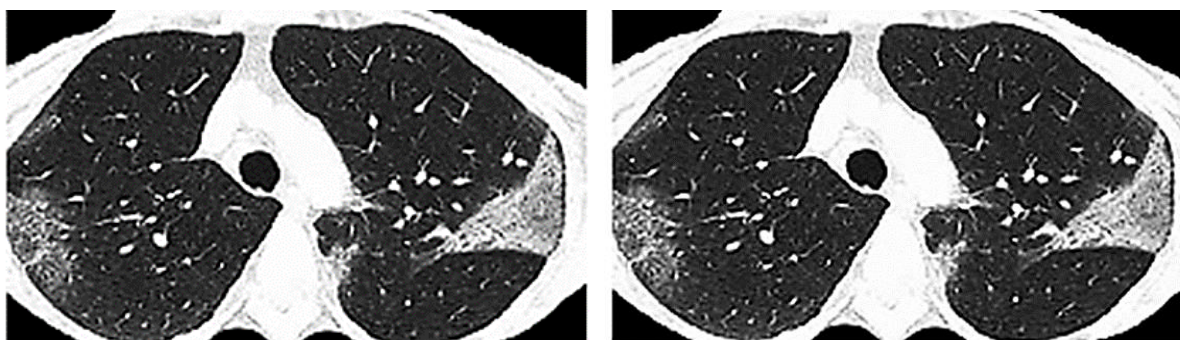
Table 2. CT images testing data sets

Classified of detection	Kaggle website	Al-Marjahn hospital	Total
Normal	150	50	200
Infected	8	2	10

3.1. Pre-processing stage

The pre-processing stage consists 4 steps to improve the CT image, as well for its preparations for the retail stage to extract COVID-19 region which is (image format conversion, grayscale image, image enhancement, and noise filtering). In this paper gray scale image has been done by function (rgb2gray) to convert RGB images to grayscale images as shown in rgb2gray scale converted code in MATLAB. The function rgb2gray has been converted RGB images to a grayscale images range (0 to 255) as shown in Figure 3(a) and Figure 3(b). In this step every the image computation because the colorful image show one

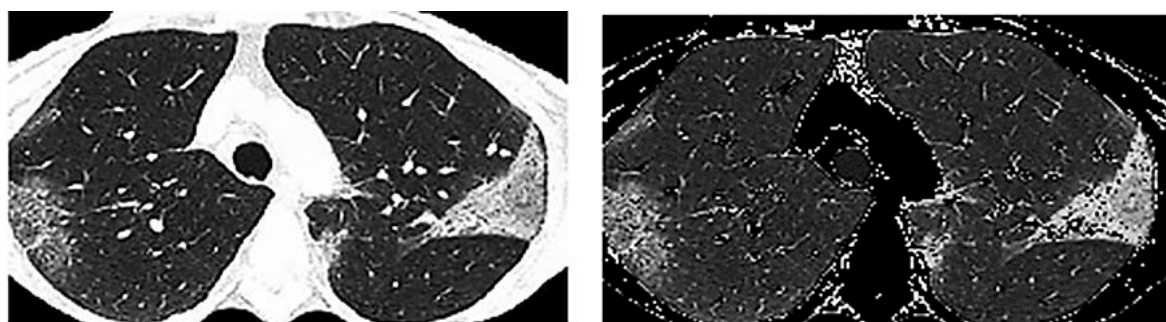
matrix while the gray image shows one. Additionally, the process of selecting a region growing level becomes easy. Then image enhancement step, in this step, the visibility and brightness of the image is improved. Figure 4(a) and Figure 4(b) shows enhancement processing for CT lung image. The final step is noise filtering in a pre-processing stage in which the extra and useless parts of CT image are removed and that anisotropic filter is applied to the image by 8-connected neighborhood for removing noise from it as show in Figure 5(a) and Figure 5(b). Table 3 show results of test anisotropic filtering works by adding noise (Gaussian noise) to CT input images and remove or deleting noise from images by anisotropic filtering using random noise value.



(a)

(b)

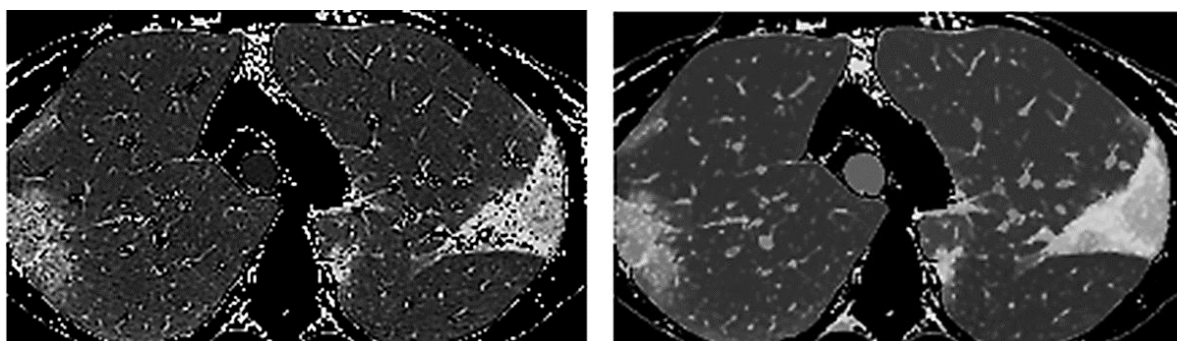
Figure 3. Image format conversion for (a) CT image for RGB and (b) CT image for gray scale



(a)

(b)

Figure 4. Image enhancement for: (a) grayscale image and (b) image enhancement


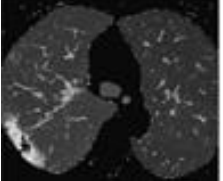
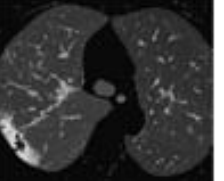

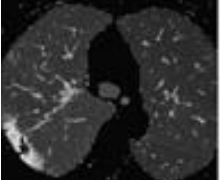
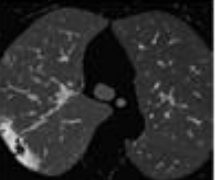

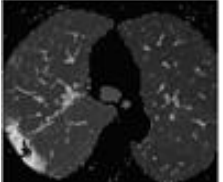
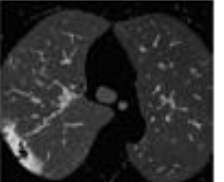


(a)

(b)

Figure 5: The noise remove CT images: (a) input ct lung image and (b) noise filtering image with anisotropic diffusion filter

Table 3. The result of test anisotropic filtering by add (Gaussian noise)

No.	Noise value	CT input image	Noisy image	Image after filtering
1	0.04			
2	0.03			
3	0.02			

3.2. Image segmentation stage

Segmentation is an image representation that is easier to parse operations as it locates the objects in the boundary and assigns a label to each pixel in the input image. The results of image segmentation consists of steps morphological operation as shown in Figure 6(a) and Figure 6(b) results the morphological processes of the CT images. The region growing algorithm segmentation gives better results due to the background of CT image are dark and the illumination is even while isolated the COVID-19 region from non-infected region. For instance, results for images are depicted in Figure 7(a) and Figure 7(b).

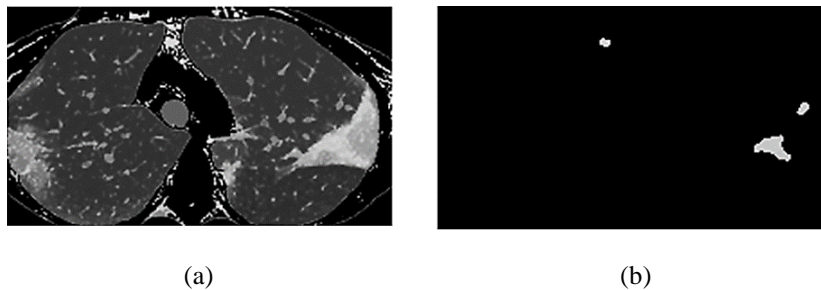


Figure 6. Experimental result of morphological operations: (a) CT image input and (b) morphological operations

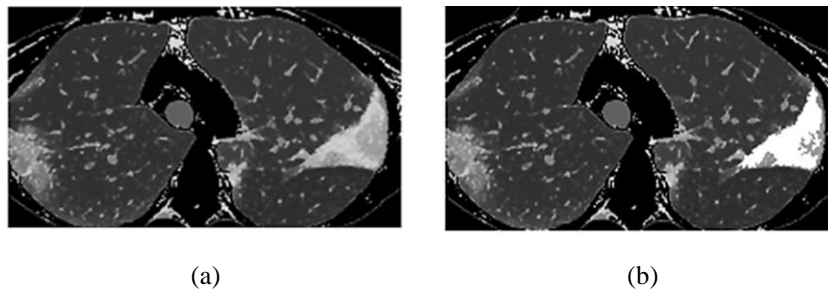


Figure 7. Experimental result of region growing segmentation: (a) CT image input and (b) proposed region growing segmentation

4. RESULTS AND ANALYSIS

The images of the trained dataset on which the extracted feature have been trained using classifier (FFBPN & SVM) for classification task, while test dataset has not trained using FFBPN & SVM classifier, only the statistical and textual feature have been extracted. The resolution training and testing image has been compared based on the COVID-19 tissue classification for FFBPN and SVM was based on COVID-19 tissue classification. Correct classification is the appropriate classification efficiency of total. The performance proposed algorithm is calculated from predictive values. There are 4 predictive values: positive true value (TP), negative true values (TN), false negative (FN) and false positive (FP) values. This has been used to measure the efficiency of CT result. Through specificity, sensitivity and precision. Feature extraction as shown in Table 4 for SVM and FFBPN.

The training FFBPN has been performed on weights and a network has been trained using neural network tool (NNTOOL). The cross-validation method has been used for training FFBPN, the data set is separated into 3 groups during each experiment, 70% of the data have been selected of the train phase, 15% of the data have been selected for validation, and the remaining 15% of the data have been used of the test phase. FFBPN pre-training and typical performance using different numbers of neurons in the hidden layer. 2, 3, and 5 neuron of the hidden layers have been selected as good number after employ several training processes of FFBPN using trial and error method.

We obtained three neuron as an ideal number used for hidden layers. FFBPN gave 99.93% accuracy of the training data set 99.99% and 76.23% accuracy is recorded testing and validation data set. Where overall method accuracy is unanimously 96.25%. Specific accuracy is only observed in 31 epochs. Figure 8, Figure 9, and Figure 10 shows performance of the system.

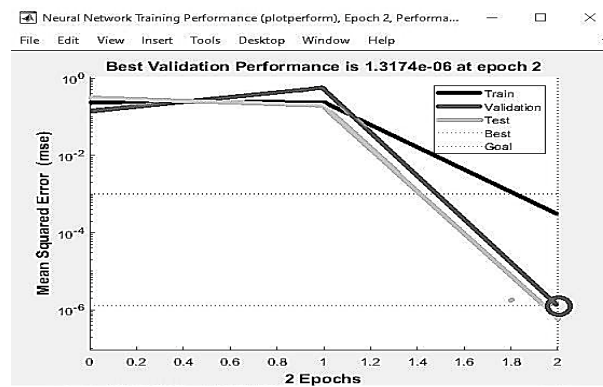


Figure 8. Typical performance of FFBPN training

Table 4. Feature extraction

	Contrast	Correlation	Energy	Homogeneity	Mean	Standard deviation	Entropy	RMS	Kurtosis	Skewness
Z1	0.1855	0.8881	0.9215	0.9916	0.064	0.333	0.0505	0.2298	30.8554	5.3311
Z2	0.2369	0.8863	0.9292	0.9917	0.0687	0.3689	0.0442	0.2111	30.3273	5.3372
Z3	0.1524	0.9493	0.8859	0.9894	0.1026	0.4288	0.0697	0.2544	17.9146	4.0592
Z4	0.1547	0.8607	0.9649	0.9959	0.0365	0.2789	0.023	0.1481	61.9089	7.7136
Z5	0.0524	0.918	0.9768	0.9978	0.0216	0.2039	0.0161	0.0585	93.8541	9.5355
Z6	0.1743	0.8444	0.9547	0.9927	0.0386	0.2739	0.0286	0.165	56.6426	7.3247
Z7	0.1487	0.8554	0.9624	0.9944	0.0344	0.264	0.0247	0.1531	65.8088	7.908
Z8	0.1389	0.93	0.9166	0.9919	0.0723	0.3558	0.0515	0.2241	26.1601	4.911
Z9	0.1408	0.8551	0.9715	0.9965	0.0306	0.2626	0.0181	0.1435	77.526	8.6806
Z10	0.3176	0.8838	0.8873	0.9839	0.0984	0.4194	0.0663	0.25	19.3913	4.1962
Z11	0.1454	0.936	0.907	0.9911	0.0815	0.3782	0.0566	0.2328	22.7828	4.5814
Z12	0.0768	0.9056	0.9546	0.9943	0.0313	0.2284	0.0303	0.1714	65.9464	7.8496
Z13	0.2371	0.9189	0.899	0.9899	0.0963	0.4257	0.0614	0.2322	19.8921	4.2961
Z14	0.1634	0.8544	0.964	0.9952	0.0363	0.2775	0.0239	0.1527	61.8227	7.7158
Z15	0.2931	0.8587	0.9232	0.9887	0.0696	0.3656	0.0476	0.2179	29.3099	5.2365
A1	0	0	1	1	0	0	0	0	0	0
A2	0	0	1	1	0	0	0	0	0	0
A3	0	0	1	1	0	0	0	0	0	0
A4	0	0	1	1	0	0	0	0	0	0
A5	0	0	1	1	0	0	0	0	0	0
A6	0	0	1	1	0	0	0	0	0	0
A7	0	0	1	1	0	0	0	0	0	0
A9	0	0	1	1	0	0	0	0	0	0

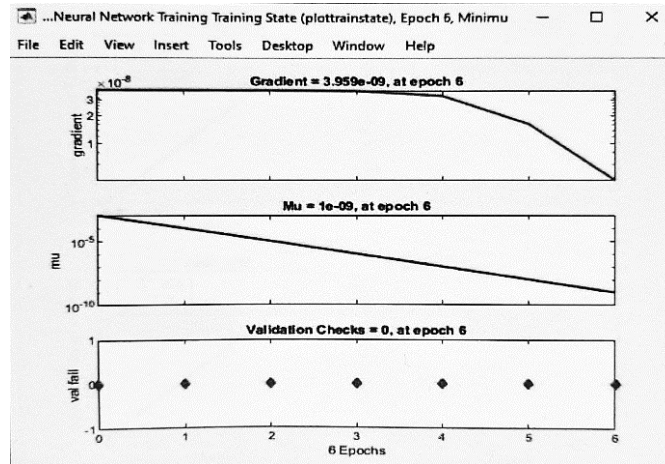


Figure 9. Plot training case of best 10 features for data

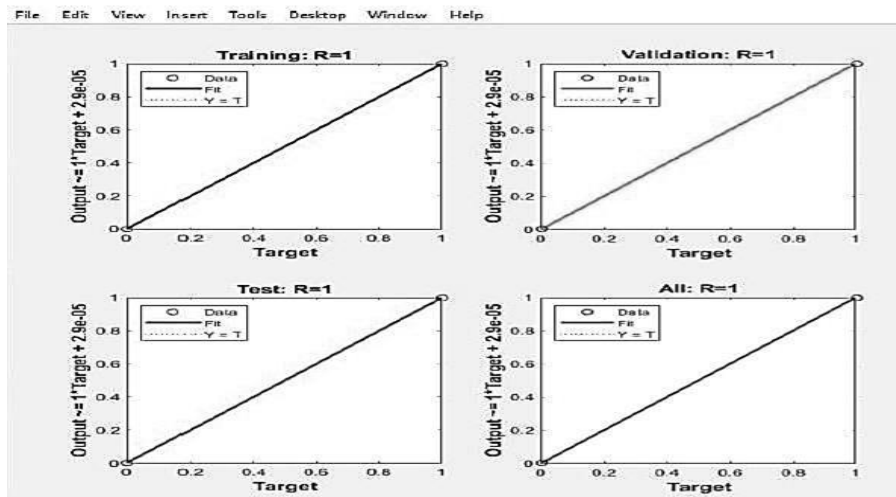


Figure 10. (Validation and training), (testing and overall) regression depicting the relationship between targets and output

5. HARDWARE IMPLEMENTATION

The Raspberry panel is one electronic chip containing computer components. The components of the practical devices are five light emitting diodes (LEDs), Raspberry, bread board and connecting cables, Raspberry shown in Figure 11. Specification of type this Raspberry (Broad-com BCM -2837B0, (32GB eMMC Flash memory devices). Setting of Raspberry Pi as following steps:

- After connecting the power cable and the ethernet cable to the computer, the Raspberry program that was previously downloaded on the computer will open (mobaxtem), the program interface will appear, double click on the IP =192.168.1.78
- Then it will ask for login as: pi
- Then it asks for password: 123
- pi@raspbary pi:~\$lsession
- After that the Raspberry interface opens and the COVID-19 program is opened, then the Raspberry program file is opened showing the result, the code interface appears, press run.
- Then we run the MATLAB program version6.mlapp, the graphical interface of the program will appear, we press open to download the CT image, then press process to start the image processing process, then the image diagnosis appears, and we notice that the Raspberry displays using LEDs what was displayed using the MATLAB interface. This program read the result as a text file and open a LED according to results by Raspberry Pi illustrate in Figure 12 and Figure 13, Table 5 illustrate results the Raspberry Pi displays using LEDs.

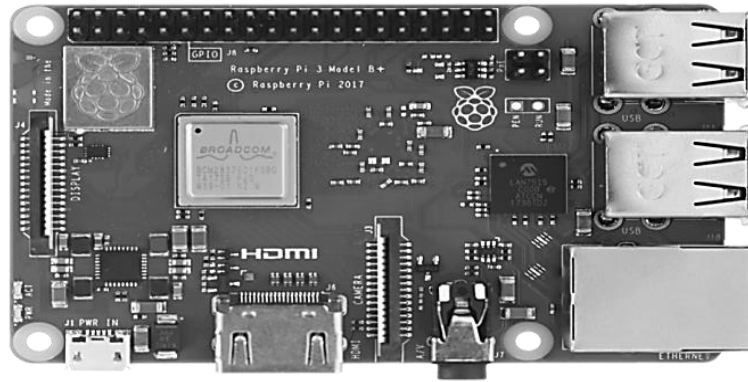


Figure 11. Raspberry Pi



Figure 12: A case of COVID-19 diagnosed with mid severity (LED yellow)



Figure 13: A case of COVID-19 diagnosed with low severity (LED blue)

Table 5. Results the Raspberry Pi displays using LEDs

Diagnosis	Green	Red	Brown	Yellow	Blue
Non-COVID-19	On	Off	Off	Off	Off
COVID-19 - high severity	Off	On	On	Off	Off
COVID-19 - mid severity	Off	On	Off	On	Off
COVID-19 - low severity	Off	On	Off	Off	On

6. CONCLUSIONS

Filter noise removal gives good preset results for removing noise from digital images in the pre-processing stage. Enhancement techniques are used to improve image information, obtain accurate results, increase image brightness, and improve image visibility, which have been made for improving the quality for the CT image. The MATLAB function (imadjust) has been used that makes image contrast with setting the value of the input density image to new value so which the data has saturated with high and low density for the inputs data. The segmentation of the lung infection area using the region growing method gave good results for detecting COVID-19. Statistical characteristics analysis is used to extract feature from image. graycomatrix computed features based on GLCM for image. The best features are used as input parameters for the back propagation network, after which the network is trained and its performance evaluated. FFBN gave good results for detection and classification COVID-19. The results showed that the noise cancellation technology using anisotropic filtering gave the best results. As for the optimization technology, only the brightness of the images has been increased. At the stage of segmentation of the area of lung infection using the region growing method, the best results are the detection of COVID-19 from other healthy. The FFBN has given the best results for detecting and classifying COVID-19 as well as determining whether a person has been infected or not. Results the hardware implementation of the Raspberry pi are give best match with software results.

ACKNOWLEDGEMENTS

I would like to express deep thanks for Al-Marjahn hospital, Babil for helping me complete the research.




REFERENCES

- [1] F. Wu *et al.*, "A new corona virus associated with human respiratory disease in China," *Nature*, vol. 579, no. 7798, pp. 265-269, Mar. 2020, doi: 10.1038/s41586-020-2008-3.
- [2] C. Huang *et al.*, "Clinical features of patients infected with 2019 novel coronavirus in Wuhan, China," *The Lancet*, vol. 395, no. 10223, pp. 497-506, Feb. 2020, doi: 10.1016/s0140-6736(20)30183-5.
- [3] Y. M. Arabi, S. Murthy, and S. Webb, "COVID-19: A novel coronavirus and a novel challenge for critical care," *Journal of Intensive Care Medicine*, vol. 46, no. 5, pp. 833-836, May 2020, doi: 10.1007/s00134-020-05955-1.
- [4] Z. Wu and J. M. McGoogan, "Characteristics of and important lessons from the coronavirus disease 2019 (COVID-19) outbreak in China: summary of a report of 72 314 cases from the chinese center for disease control and prevention," *Journal of JAMA*, vol. 323, no. 13, pp. 1239-1242, Apr. 2020, doi: 10.1001/jama.2020.2648.
- [5] M. L. Holshue *et al.*, "First case of 2019 novel coronavirus in the United States," *The New England Journal of medicine*, vol. 382, no.10, pp. 929-936, Jan. 2020, doi: 10.1056/NEJMoa2001191.
- [6] W. Kong and P. P. Agarwal, "Chest imaging appearance of COVID-19 infection," *Radiology*, vol. 2, no. 1, 2020, doi: 10.1148/ryct.2020200028.
- [7] Ö. Özdemir, "Coronavirus Disease 2019 (COVID-19): Diagnosis and Management," *Erciyes Medicine Journal*, vol. 42, no. 3, pp.242-7, 2020, doi: 10.14744/etd.2020.99836.
- [8] M. Anthimopoulos, S. Christodoulidis, L. Ebner, A. Christe and S. Mougiakakou, "Lung Pattern Classification for Interstitial Lung Diseases Using a Deep Convolutional Neural Network," in *IEEE Transactions on Medical Imaging*, vol. 35, no. 5, pp. 1207-1216, May 2016, doi: 10.1109/TMI.2016.2535865.
- [9] Y. Wang *et al.*, "Precise pulmonary scanning and reducing medical radiation exposure by developing a clinically applicable intelligent CT system: Towards improving patient care," *EBioMedicine*, vol. 54, p. 102724, 2020, doi: 10.1016/j.ebiom.2020.102724.
- [10] K. Buys, C. Cagniart, A. Baksheev, T. D. Laet, J. D. Schutter, and C. Pantofaru, "An adaptable system for RGB-D based human body detection and pose estimation," *Journal of Visual Communication and Image Representation*, vol. 25, no. 1, pp. 39-52, 2014, doi: 10.1016/j.jvcir.2013.03.011.
- [11] D. Selvaraj, A. Venkatesan, V. G. V. Mahesh, and A. N. J. Raj, "An integrated feature frame work for automated segmentation of COVID-19 infection from lung CT images," *International Journal of Imaging Systems and Technology*, vol. 31, no. 1, pp. 28-46, 2020, doi: 10.1002/ima.22525.
- [12] J. Sutherland *et al.*, "Applying modern virtual and augmented reality technologies to medical images and models," *Journal of digital imaging*, vol. 32, no. 1, pp. 38-53, Feb. 2019, doi: 10.1007/s10278-018-0122-7.
- [13] N. Goel, A. Yadav, and B. M. Singh, "Medical image processing: A review," *2016 Second International Innovative Applications of Computational Intelligence on Power, Energy and Controls with their Impact on Humanity (CIPECH)*, 2016, pp. 57-62, doi: 10.1109/CIPECH.2016.7918737.




- [14] Z. Cao, T. Simon, S. E. Wei, and Y. Sheikh, "Realtime multi-person 2d pose estimation using part affinity fields," In *Proceedings of the IEEE Conference on Computer Vision and Pattern Recognition*, pp. 7291-7299, 2017. [Online]. Available: https://openaccess.thecvf.com/content_cvpr_2017/papers/Cao_Realtime_Multi-Person_2D_CVPR_2017_paper.pdf
- [15] M. Diwakar and M. Kumar, "A review on CT image noise and its denoising," *Biomedical Signal Processing and Control*, vol. 42, pp. 73-88, Apr. 2018, doi: 10.1016/j.bspc.2018.01.010.
- [16] Y. Li and L. Xia, "Coronavirus disease 2019 (COVID-19): Role of chest ct in diagnosis and management," *American Journal of Roentgenology*, vol. 214, no. 6, pp.1280-1286, 2020, doi: 10.2214/ajr.20.22954.
- [17] X. Xie, Z. Zhong, W. Zhao, C. Zheng, F. Wang, and J. Liu, "Chest CT for typical coronavirus disease 2019 (COVID-19) pneumonia: relationship to negative RT-PCR testing," *Radiology*, vol. 296, no. 2, pp. E41-E45, 2020, doi: 10.1148/radiol.202000343.
- [18] S. Salehi, A. Abedi, S. Balakrishnan, and A. Gholamrezanezhad, "Coronavirus disease 2019 (covid-19): A systematic review of imaging findings in 919 patients," *American Journal of Roentgenology*, vol. 215, no.1, pp. 87-93, Mar. 2020. doi: 10.2214/ajr.20.23034.
- [19] S. Khobragade, A. Tiwari, C. Y. Patil, and V. Narke, "Automatic detection of major lung diseases using Chest Radiographs and classification by feed-forward artificial neural network," *2016 IEEE 1st International Conference on Power Electronics, Intelligent Control and Energy Systems (ICPEICES)*, 2016, pp. 1-5, doi: 10.1109/ICPEICES.2016.7853683.
- [20] K. A. Prayogo, A. Suryadibrata, and J. C. Young, "Classification of pneumonia from X-ray images using siamese convolutional network," *TELKOMNIKA (Telecommunication Computing Electronics and Control)*, vol. 18, no. 3, pp.1302-1309, Jun. 2020, doi: 10.12928/TELKOMNIKA.v18i3.14751.
- [21] A. I. Khan, J. L. Shah, and M. M. Bhat, "CoroNet: A deep neural network for detection and diagnosis of COVID-19 from chest x-ray images," *Computer Methods and Programs in Biomedicine*, vol. 196, no. 105581, 2020, doi: 10.1016/j.cmpb.2020.105581.
- [22] Z. T. Al-Ars and A. Al-Bakry, "A web/mobile decision support system to improve medical diagnosis using a combination of K-Mean and fuzzy logic," *TELKOMNIKA (Telecommunication Computing Electronics and Control)*, vol. 17, no. 6, pp. 3145-3154, Dec. 2019, doi: 10.12928/TELKOMNIKA.v17i6.12715.
- [23] M. S. Croock, S. D. Khuder, A. E. Korial, and S. S. Mahmood, "Early detection of breast cancer using mammography images and software engineering process," *TELKOMNIKA (Telecommunication Computing Electronics and Control)*, vol. 18, no. 4, pp. 1784-1794, Aug. 2020, doi: 10.12928/TELKOMNIKA.v18i4.14718.
- [24] M. V. Enriquez, "A Deep Learning Approach for Pneumonia Detection on Chest X-Ray," M.sc, Thesis, Telecommunications Engineering, University of Vigo [Online]. Available: <http://castor.det.uvigo.es:8080/xmlui/bitstream/handle/123456789/400/TFM%20Manuel%20V%C3%A1lquez%20Enr%C3%ADquez.pdf?sequence=1&isAllowed=y>.
- [25] M. Goyal, "Morphological image processing," *International Journal of Computer Science and Technology*, vol. 2, no. 4, pp. 161-165, 2011. [Online]. Available: <http://www.ijcst.com/vol24/1/megha.pdf>

BIOGRAPHIES OF AUTHORS



Nawres Aref Alwash    B.sc at Electronic and Communication Engineering University of Technology Baghdad, Iraq 2000, M. Sc Electronic Engineering University of Technology Baghdad, Iraq 2021. He can be contacted at email: eee.19.18@grad.uotechnology.edu.iq.



Dr. Hussain Kareem Khleaf    B. Sc at Electronic and Communication Engineering University of Technology Baghdad, Iraq 2001, M. Sc Electronic Engineering University of Technology Baghdad, Iraq 2003, Ph. D Biomedical Engineering University Malaysia Pahang (UMP) Malaysia, Pahang 2015. He can be contacted at email: 30068@uotechnology.edu.iq.